

“What is ‘liquid’? Understanding the states of matter”

By LJ. MILANOVIĆ, H. A. POSCH

Institut für Experimentalphysik, Universität Wien, Boltzmannngasse 5,
A-1090 Vienna, Austria

and WM. G. HOOVER

Department of Applied Science, University of California at Davis/Livermore and
Lawrence Livermore National Laboratory, Livermore, CA 94551-7808, USA

(Received 12 December 1997; accepted 8 January 1998)

Molecular dynamics answers the question “what is ‘liquid’?” by describing the detailed dynamic structure of simulated liquids in the many-dimensional phase space of statistical mechanics. The Lyapunov instabilities of liquid motion reveal collective dynamic modes, quite unlike those of solid state studies, superimposed on the van der Waals hard particle static structure. Here we illustrate these developments in the characterization of ‘liquid’ with examples from our recent dynamic instability studies of two-dimensional dumbbell fluids.

1. Introduction

John Barker [1], with considerable help from Doug Henderson, devoted more than 30 years to the question “What is ‘liquid’?” [2]. We adopt their title here as the motivating question underlying our own work. For John, it was a lifelong fascination: finding the interatomic and intermolecular forces, models, and simulation techniques which could reproduce first qualitatively, but ultimately quantitatively, liquid properties. Condensed rare gases were a recurring subject in his studies. His work spanned the transition from crude mechanical liquid-structure models (Bernal’s aggregates of steel ball bearings [3] and Hildebrand’s coloured gelatin spheres [4], suspended in a fish tank, come to mind) to the computer simulations of liquid structure which are commonplace today. In their early work on liquid perturbation theory, Barker and Henderson discovered that the van der Waals hard sphere picture provided a workable structural model for computing static liquid properties. Liquid free energies, suitable for thermodynamic calculations, could be estimated by finding the density and temperature dependence of the optimum hard sphere diameter.

Though diffraction experiments provided pair distribution functions, without further guidance from computer simulations liquid structure would have remained mysterious. Molecular dynamics and Monte Carlo simulations are by now a routine activity for thousands of simulators worldwide. Barker was an active participant in developing this work at IBM. The first computer

simulations emphasized static properties, the mechanical and thermal equations of state and phase coexistence. The non-equilibrium dynamics of liquids, including hydrodynamic flows, and shockwaves, had to await more powerful computers. Today the largest simulations involve 10^8 individual atoms.

van der Waals’ picture of a structure dominated by hard sphere forces, but softened by weak attractions, has changed very little. The perturbation theory calculations showed that a smooth short-range caricature of the long-range Lennard-Jones force law provides a quantitatively useful picture of fluid structure. Liquid structure is not very different from that illustrated by Alder and Wainright in their 1959 *Scientific American* article [5]. The early models which had developed, prior to these simulations, described dense fluids in terms of cell free volumes, or ‘significant structures’, a mix of gaslike and solidlike degrees of freedom. The inclusion of free flight or unstable motions to distinguish a fluid from a solid made good sense, as did the inclusion of ‘holes’. But a search for these holes revealed their absence, and computer studies of the free path distribution showed that liquids and solids are not so different [6, 7].

What does distinguish a liquid from a solid? It is the ability to flow, which is collective. What distinguishes between equilibrium and non-equilibrium liquids? One might hope to see hints of these differences in the many-body representations of phase space dynamics, which are just now becoming available. This more detailed view, inaccessible to experiment, allows us to probe

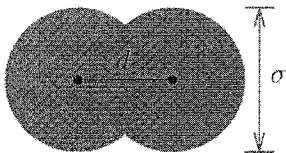


Figure 1. Geometry of a hard dumbbell.

the effect of *perturbations* of the many-body state in phase space [8–14]. The idea is to discover these directions in phase space in which the flow is most rapidly diverging. These are the instabilities that characterize a liquid state. The contracting directions, required by the time-reversibility of the equations of motion, are paired with the expansions. These instabilities may be studied by computing the set of Lyapunov exponents, defined as the time-averaged exponential rates of divergence (convergence) of infinitesimal perturbations of phase space states. In the remainder of this paper we apply such an analysis to a simple model of a molecular fluid in two dimensions: a system of N planar hard dumbbells. Each dumbbell is made up of two overlapping discs, as shown in figure 1, and the total phase space is $6N$ -dimensional. The price of this more general exploration of the question “What is ‘liquid?’” is that $6N(6N + 1)$ differential equations must be solved instead of the $6N$ motion equations for the original state variables. The upcoming advances in computer power will enable a comprehensive exploration of these ideas in the next decade.

2. Hard dumbbell fluid model

Hard disc dynamics proceeds by checking the developing trajectories for overlaps backing up to the precise time of each collision, and then continuing [15]. ‘Smooth’ hard dumbbells were studied by Bellemans, Orban and Van Belle [16]. These ‘molecules’ exert impulsive forces exactly normal to their surfaces and are a generalization of this model which retains the simplicity of isolated impulsive collisions. Each dumbbell is formed by two rigidly connected hard discs of diameter σ with centre to centre separation d . Collisions conserve both total and angular momentum through strictly normal forces. The total molecular mass m is assumed to be homogeneously distributed over the union of the two discs, resulting in a moment of inertia explicitly given in [17]. In our numerical work we use reduced units for which the disc diameter σ , the molecular mass m , and the specific energy $E/N = K/N$ are equal to unity. The unit of time is $(m\sigma^2 N/K)^{1/2}$, where K is the total kinetic energy of the system. The molecular anisotropy d/σ is simply denoted by d . The number density of the system is defined by $n = N/V$, where V is the area of the simulation box.

The state of an N -dumbbell system is given by the $6N$ -dimensional vector $\Gamma = \{\mathbf{r}_i, \mathbf{p}_i, \alpha_i, J_i; i = 1, \dots, N\}$, where \mathbf{r}_i and \mathbf{p}_i are the centre of mass position and linear momentum of molecule i , and α_i and J_i denote the orientation angle and the angular momentum for rotation around its centre of mass, respectively. The Lyapunov exponents are defined by

$$\lambda(\delta\Gamma(0)) = \lim_{t \rightarrow \infty} \frac{1}{t} \ln \frac{|\delta\Gamma(t)|}{|\delta\Gamma(0)|}, \quad (1)$$

where the vector $\delta\Gamma(t)$ gives the infinitesimal displacement of a perturbed satellite trajectory from the reference trajectory $\Gamma(t)$. There are $6N$ orthonormal initial offset vectors $\delta\Gamma_l(0)$ yielding a set of exponents $\{\lambda_l\}$, $l = 1, \dots, 6N$. This set, the so-called Lyapunov spectrum, is taken to be ordered such that $\lambda_l \geq \lambda_{l+1}$. In a recent paper [17] we have outlined our method for computing the Lyapunov spectra of two-dimensional dumbbell fluids, and have summarized the general properties of such spectra. There we have concentrated on low-density gases. Here we present analogous results for higher densities, both below and above the fluid-to-solid phase transition.

All our simulations are carried out in equilibrium states. Although the present results are exploratory, they establish that the two-dimensional dumbbell model has no difficulty reaching an equilibrium, even in small systems with relatively small aspect ratios. The partition of kinetic energy between the rotational and translational modes is typically within half a per cent of the equipartition value. It was verified numerically that, for vanishing total momentum, $K_{\text{trans}} = (2N - 2)K/(3N - 2)$, where K_{trans} is the kinetic energy of the translational modes.

3. Simulation results for the Lyapunov instability

Figure 2 summarizes the dependence of the Lyapunov spectrum for a 64-dumbbell system on the molecular anisotropy. The density $n = 0.5\sigma^{-2}$, well below the phase transition density. Only the positive branch, related to phase-space expansion, of each spectrum is shown. On the abscissa the Lyapunov exponents are labelled by the index l , where $l = 1$ refers to the maximum, and $l = 3N - 3 = 189$ to the smallest positive exponent. Three out of the six vanishing exponents for each spectrum [17], $\lambda_{190} - \lambda_{192}$, also are accounted to the positive branch. Most prominent in the figure is a step in the spectra between $l = 2N - 3 = 125$ and $l = 126$, if the molecular anisotropy is smaller than a critical anisotropy, $d/\sigma < d_c/\sigma \approx 2^{-4}$. It separates each spectrum into a translational part, $1 \leq l \leq 2N - 3 = 125$, and a rotational part, $126 \leq l \leq 189$, dominated by the translational and rotational degrees of freedom, respectively. Depending on l , the offset vectors associated with the

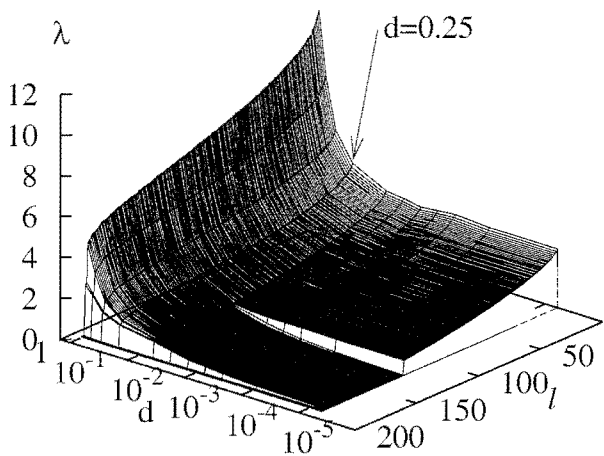


Figure 2. Lyapunov spectra for a fluid of 64 hard dumbbells at a number density $0.5/\sigma^2$ and various anisotropies d/σ . Only the positive branch with $3 \times N = 192$ exponents for each spectrum is shown.

exponents λ_l point, in the course of time, predominantly into one of the two subspaces spanned by the variables belonging either to centre of mass translation or molecular reorientation, and rarely rotate into a direction belonging to the other subspace [17]. For anisotropies $d > d_c$, however, one finds that the offset vectors for all exponents spend a comparable time in both subspaces, which is taken as an indication of strong coupling between translational and rotational degrees of freedom. d_c is found to increase with the density. The dependence of some selected Lyapunov exponents on the molecular anisotropy is shown in figure 3 for the density $n = 0.5\sigma^{-2}$. The horizontal lines for $l = 1$ and $l = 2N - 3 = 125$ indicate the maximum and smallest

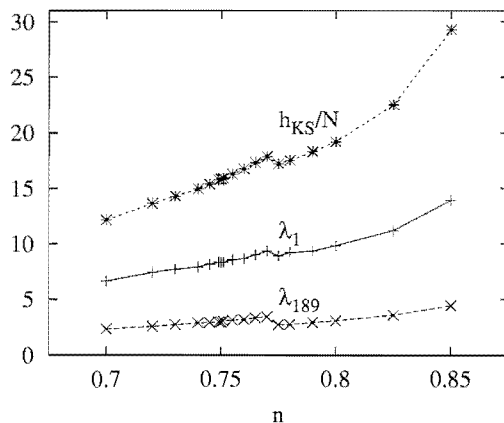


Figure 4. Density dependence of the maximum exponent λ_1 , the smallest positive exponent λ_{189} , and the Kolmogorov-Sinai entropy per particle h_{KS}/N , for a 64-dumbbell system with anisotropy $d/\sigma = 0.25$. The number density is measured in units of σ^{-2} , and the displayed quantities in units of $[(K/N)/m\sigma^2]^{1/2}$.

positive exponents of a 64-disc system in two dimensions, taken from [18], to which the respective exponents of the dumbbell system converge with $d \rightarrow 0$ [17]. For the following considerations we restrict ourselves to a molecular anisotropy $d/\sigma = 0.25$ belonging to the roto-translational regime.

The variation of the maximum and smallest positive exponents with density is shown in figure 4 for a 64-dumbbell system with $d/\sigma = 0.25$. Also shown is the Kolmogorov-Sinai entropy per molecule, h_{KS}/N . For closed systems h_{KS} is, according to Pesin's theorem [19], the sum of the positive Lyapunov exponents. One observes a step in these curves near $n = 0.775\sigma^{-2}$, which corresponds to a transition from an ordered state, with orientational disorder, to a crystalline state with long-range orientational order. This may be deduced from the orientational correlation functions $\langle \cos(\Theta) \rangle$ shown in figure 5 for a number of densities, where Θ is the angle of reorientation of an arbitrary molecule during a time t . The steps persist if, instead of the density n , the measured collision frequency is used on the abscissa of figure 4. The transition from a fluid to an orientationally disordered solid takes place near the density $n = 0.75\sigma^{-2}$. It makes itself felt by large fluctuations of the exponents and slow convergence. However, because of the small number of particles, this transition is too gradual to leave any noticeable trace in the density dependence of the Lyapunov exponents. The coupling between translational and rotational degrees of freedom also affects this phenomenon. For the purely translational case of 64 planar discs we found previously [18] that a significant step in the density dependence of the maximum exponent is observed at the fluid-to-solid transition density, which is due mainly to the change

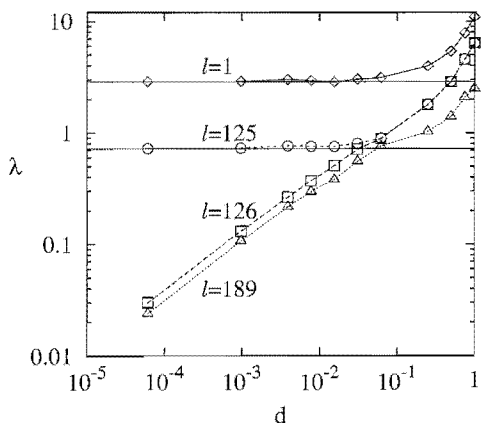


Figure 3. Anisotropy dependence of selected positive Lyapunov exponents, labelled by their index l , for a 64-dumbbell system of density $n = 0.5\sigma^{-2}$. d is given in units of the disc diameter σ , and the λ_l in units of $[(K/N)/(m\sigma^2)]^{1/2}$. The horizontal lines indicate the values of corresponding exponents for a gas of 64 hard discs.

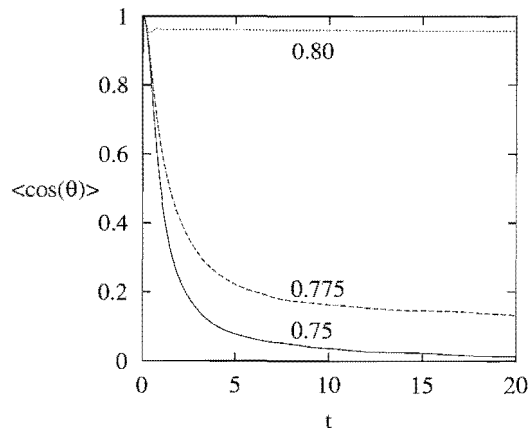


Figure 5. Orientational correlation function $\langle \cos(\theta) \rangle$ for different densities n (indicated by the labels in units of σ^{-2}) for a 64-dumbbell system with anisotropy $d/\sigma = 0.25$. The time t is measured in units of $[m\sigma^2/(K/N)]^{1/2}$.

in the collision frequency at the phase transition. It disappears if the Lyapunov exponents are viewed as a function of the collision frequency instead of the density.

The step in λ_l , indicating the locking of dumbbell orientations, is more pronounced for λ_{189} than for λ_1 . This seems to indicate that collective long-wavelength phenomena have more impact on the smallest positive than on the largest exponents, the latter being more sensitive to local short-wavelength dynamic events. Since the permitted long wavelength modes are determined by the size of the simulation cell, we compare in figure 6 various spectra for a 120-dumbbell system obtained for different aspect ratios $A = L_y/L_x$ as indicated by the labels. L_x and L_y denote the size of the box

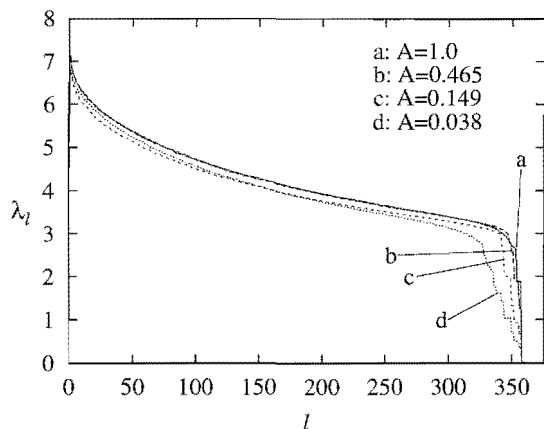


Figure 6. Lyapunov spectra for a 120-dumbbell fluid (anisotropy $d/\sigma = 0.25$, density $n = 0.7\sigma^{-2}$) for various aspect ratios L_y/L_x of the simulation cell. The exponents are defined only for integer indices l and are measured in units of $[(K/N)/m\sigma^2]^{1/2}$.

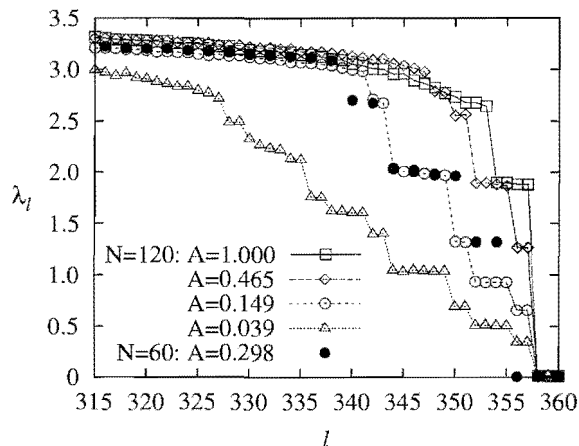


Figure 7. The spectra with the open symbols are a magnification of the smallest positive wings of the spectra displayed in figure 6. The aspect ratio A is identified by the symbols. The filled circles are Lyapunov exponents taken from a spectrum of a 60-dumbbell system with an aspect ratio $A = 0.298$. For details we refer to the main text.

in the x and the y directions, respectively. The usual periodic boundary conditions are used. The density for figure 6 is $n = 0.7\sigma^{-2}$, well in the fluid regime, and the anisotropy $d/\sigma = 0.25$. A magnified view of the spectral wing with the smallest positive exponents is presented in figure 7. From figure 6 we conclude that the largest Lyapunov exponents λ_l for indices $l < 300$ are not very sensitive to A (with the exception, perhaps, of the most extreme ratios $A < 0.15$): these exponents are a consequence of fast local dynamic events. Figure 7, however, proves that the smallest positive exponents are very sensitive to A and, hence, to the long-wavelength modes permitted by a given aspect ratio. One observes also in this figure a twofold degeneracy of a few of the smallest positive exponents. The underlying symmetry will be discussed below.

The spectra with the open symbols in figure 7 are all for a system containing 120 dumbbells. We have superimposed the spectrum with $A = 0.149$ (open circles) on a spectrum for a 60-dumbbell system with the same particle density and an aspect ratio $A = 0.298$. Thus, the width of the simulation box in the y direction is the same for both systems. Since the smaller system has only half as many exponents, its indices l have been doubled to represent the exponents (by the filled circles) in figure 7. One observes that all exponents of the smaller system correspond to equivalent exponents in the larger system (circles). The latter is distinguished only by the fact that *additional* exponents appear in the spectrum which are sensitive to modes in x direction permitted only in the larger of the two systems.

It might be expected that the expansion in certain phase space directions would be dominated by whichever pair of dumbbells was colliding. But because the directions depend upon the past history of the motion, collective modes develop, which affect the various exponents in a selective way. To visualize these modes we have introduced projections of the phase-space offset vectors $\delta\mathbf{F}_i$, associated with the exponents λ_i , into the subspaces μ_i spanned by the state variables of the individual molecules i [17, 20]. The sum of all square components contributed by such a molecule is referred to as the ‘squared particle component’ $\delta_{\mu_i,l}^2(t)$. Summed over all particles the squared components obey $\sum_{i=1}^N \delta_{\mu_i,l}^2(t) = 1$. As the offset vector $\delta\mathbf{F}_i$ reorients in phase space, the squared particle components vary with time. They indicate to what extent the various molecules contribute to the expansion (contraction) process, quantified by the corresponding Lyapunov exponents, in phase space at any instant of time. In figure 8(a–c) individual dumbbells are marked according to their square particle components. The central part of a dumbbell is black if its squared component associated with a selected Lyapunov exponent exceeds a certain threshold, $\delta_{\mu_i,l}^2 > A^2$. Similarly, the peripheral boundary of a molecule is grey if its component pertaining to *another* specified exponent fulfils an analogous criterion.

Figure 8(a–c) shows three versions of a single equilibrium configuration for a 120-dumbbell system with aspect ratio $A = 1$. Let us first discuss figure 8(a), in which the black centres indicate those molecules contributing most to the maximum exponent λ_1 . It is observed that the marked dumbbells are very localized in space, which shows that there is only a small active zone contributing to the fastest growth in any direction of phase space. All the other molecules contribute hardly at all to λ_1 at this instant of time [17, 20]. The localization is a consequence of the fact that two colliding molecules have a chance to contribute significantly to λ_1 only if their offset-vector components are already far above average before the collision. Furthermore, the renormalization procedure for the offset vector $\delta\mathbf{F}_1$, required for the computation of the maximum exponent [21, 22], tends to suppress the components of non-colliding particles. Taken together, these two mechanisms favour the colliding molecules with the largest components. It is interesting to note that this behaviour is reproduced by the ‘clock model’ of van Zon *et al.* [23], introduced for the computation of the maximum exponent of a hard sphere gas.

An even more interesting situation arises for the four smallest positive exponents $\lambda_{354}, \dots, \lambda_{357}$, for which the contributing modes are visualized in figure 8(b) (λ_{354} , black centre; λ_{355} , grey boundary) and figure 8(c) (λ_{356} , black centre; λ_{357} , grey boundary). The figures

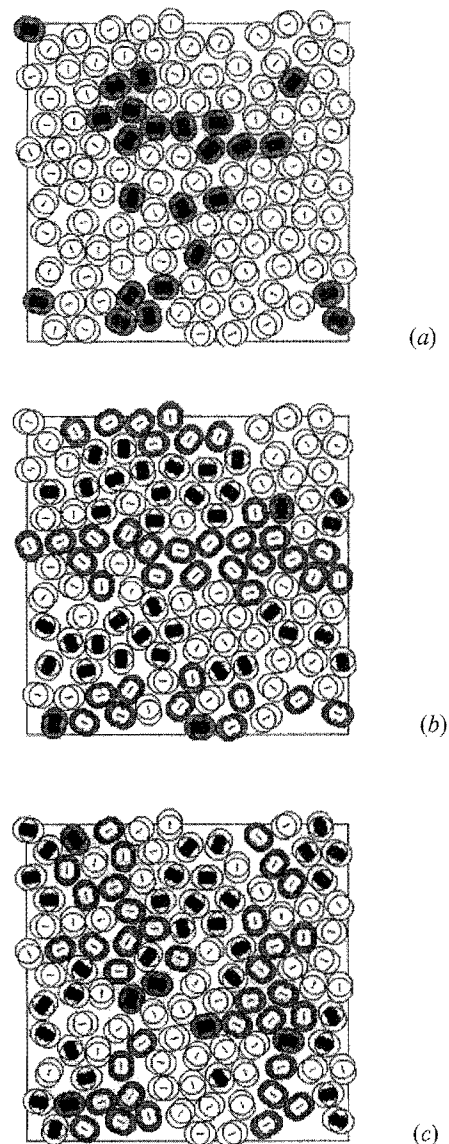


Figure 8. Snapshot of a 120-dumbbell fluid in equilibrium at a density of $n = 0.7\sigma^{-2}$ and aspect ratio $A = 1$. The molecular anisotropy $d/\sigma = 0.25$. The dumbbells are marked according to their square particle components $\delta_{\mu_i,l}^2$ introduced in the main text, where the following criteria apply: (a) $\delta_{\mu_i,1}^2 > 0.01$, black centre; (b) $\delta_{\mu_i,354}^2 > 0.01$, black centre, $\delta_{\mu_i,355}^2 > 0.01$, grey boundary; and (c) $\delta_{\mu_i,356}^2 > 0.01$, black centre, $\delta_{\mu_i,357}^2 > 0.01$, grey boundary.

reveal a coherent mode structure, arranged horizontally in part (a), and vertically in part (b), but otherwise very similar for all four exponents. So it does not come as a surprise that these exponents turn out to be equal, as may be inferred directly from the open squares in figure 7.

Another example for an aspect ratio $A = 0.149$ is provided in figures 9 and 10. There we use a slightly dif-

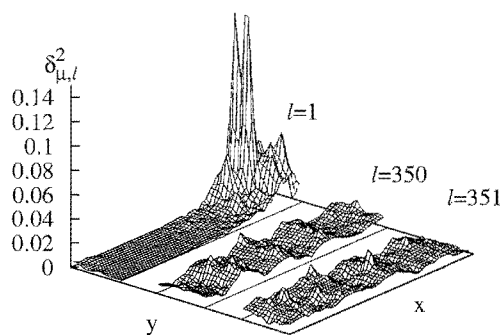


Figure 9. Surfaces of square particle exponents $\delta_{\mu,l}^2$, interpolated over regular grid points covering the simulation cell, for a snapshot of a 120-dumbbell fluid in equilibrium. The aspect ratio $A=0.149$, the number density is $n=0.7\sigma^{-2}$, and the molecular anisotropy $d/\sigma=0.25$. The various surfaces are labelled by their Lyapunov indices l .

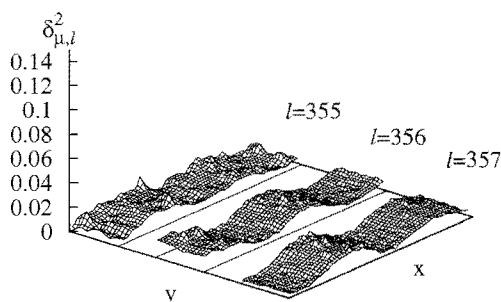


Figure 10. Snapshot of the surface of squared particle exponents $\delta_{\mu,l}^2$ for the same configuration of the 120-dumbbell fluid depicted in figure 9. The various surfaces are labelled by their Lyapunov indices l .

ferent representation which shows the mode structure even more clearly. The squared particle components $\delta_{\mu,i}^2$ for an instantaneous configuration of 120 dumbbells are interpolated for regular grid points and are plotted along the vertical axis over the grid covering the simulation box. The Lyapunov vectors and exponents related to such a $\delta_{\mu,l}^2(x,y)$ surface are labelled by their index l . In figure 9 we recognize, for $l=1$, the very localized mode structure for λ_1 , whereas the coherent structures for the exponents λ_{350} and λ_{351} resemble waves along the x axis with a wavelength $L_x/4$. According to figure 7, the four exponents $\lambda_{352}, \dots, \lambda_{355}$ are all equal. Their instantaneous mode structure, for which one example, $l=355$, is shown in figure 10, looks rather complicated and seems to involve a wave pattern in both the x and y directions. The structures for the two smallest positive exponents λ_{356} and λ_{357} , however, are very simple again and resemble waves along the x axis with a wavelength twice as long as those for $l=350$ and 351 in figure 9. According to figure 7 both exponents are also equal (see

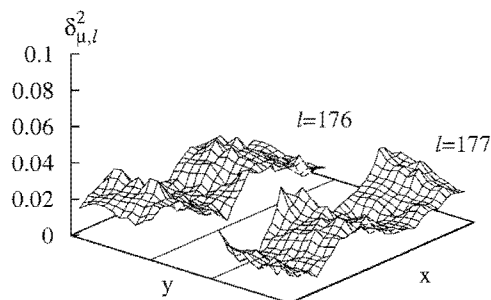


Figure 11. Surfaces of squared particle exponents $\delta_{\mu,l}^2$, interpolated over regular grid points covering the simulation cell, for a snapshot of a 60-dumbbell fluid in equilibrium. The aspect ratio $A=0.298$, the number density is $n=0.7\sigma^{-2}$, and the molecular anisotropy $d/\sigma=0.25$. The surfaces correspond to the two smallest positive exponents and are labelled by the Lyapunov indices l .

the open circles), and it comes as no surprise that their modes are also very similar.

For comparison we show in figure 11 also the modes for the two smallest positive exponents λ_{176} and λ_{177} for a 60-dumbbell system with the same number density as before, but with twice the aspect ratio, $A=0.298$. We have noted previously that these exponents, represented in figure 7 by filled circles with their Lyapunov indices multiplied by two, are practically equal to the exponents λ_{350} and λ_{351} of the 120-dumbbell system depicted in figure 9. Also, as expected, the mode structures are the same taking into account that the simulation cells differ in the x direction by a factor of two.

4. Conclusion

Characterizing liquids through their dynamic stability properties is just beginning. Our results suggest an overall structure with collective modes which can be deduced from the Lyapunov offset vectors.

Despite the adequacy of the van der Waals hard core model for the structure of 'simple' (mass-point) fluids, much remains to be done in characterizing liquids with internal degrees of freedom. We have found, unexpectedly, that the dynamic instabilities associated with collective motions, particularly the low-frequency long term modes characteristic of the smallest positive Lyapunov exponents, are coherent in both space and time. The physical nature of these modes is a real challenge for today's computers. Theoretical models, designed to reproduce the modal structures, could be based upon cell models, as well as geometrical models adopting frozen rotational or translational coordinates. Such models might be particularly useful for understanding spectral changes associated with the melting and solid-phase librational phase transitions.

The Lyapunov spectrum is formally related to the same dynamic matrix which generates the vibrational modes of solids [24], but, for fluids as well as solids, the structure is far less complex than a solid phase frequency spectrum [9]. Evidently the spatial contributions of the particles make up in complexity what the Lyapunov spectrum lacks.

The present work, in which the dependence of the Lyapunov eigenvectors on aspect ratio is considered, clearly reveals the strong influence of symmetry on the modes. This suggests exploratory calculations with dumbbell molecules on the surface of a three-dimensional sphere. It is also possible to study particular modes by using feedback control to 'steer' the reference system in the direction of particularly interesting modes.

Here we have described some of our phase-space studies of equilibrium fluids, the results so far obtained, and the conclusions and some new questions to which these lead. The non-equilibrium situation is even more complex, with a fractal phase-space structure rather than a smooth one, and is currently under active investigation. It is certainly possible to study the couplings linking shear flow, molecular alignment, and Lyapunov instability. Relaxation from highly non-equilibrium initial conditions should also lead to interesting structure in the Lyapunov spectra.

Evidently the question "What is 'liquid'?" will occupy researchers for some time. We believe that the dumbbell model and the Lyapunov eigenvectors will prove to be useful tools in the search for new understanding.

Work at the University of Vienna was supported by Grant P11428-PHY from the Fonds zur Förderung der wissenschaftlichen Forschung; work at the Lawrence Livermore National Laboratory was performed under the auspices of the University of California, through Department of Energy contract W-7405-eng-48, and was further supported by the Methods Development Group in the Department of Mechanical Engineering at the Livermore Laboratory.

References

- [1] BARKER, J. A., 1963, *Lattice Theories of the Liquid State* (Oxford: Pergamon Press).
- [2] BARKER, J. A., and HENDERSON, D., 1976, *Rev. mod. Phys.*, **48**, 587.
- [3] BERNAL, J. D., and KING, S. V., 1968, *Physics of Simple Liquids*, edited by H. N. V. Temperley, J. S. Rowlinson, and G. S. Rushbrooke (Amsterdam: North-Holland) p. 231.
- [4] HILDEBRAND, J. H., and SCOTT, R. L., 1962, *Regular Solutions* (Englewood Cliffs, NJ: Prentice Hall).
- [5] ALDER, B. J., and WAINWRIGHT, T. E., 1959, *Sci. Amer.*, **201**(4), 113.
- [6] EINWOHNER, T., and ALDER, B. J., 1968, *J. chem. Phys.*, **49**, 1458.
- [7] HOOVER, W. G., and ROSS, M., 1971, *Contemp. Phys.*, **12**, 339.
- [8] POSCH, H. A., and HOOVER, W. G., 1988, *Phys. Rev. A*, **38**, 473.
- [9] POSCH, H. A., and HOOVER, W. G., 1989, *Phys. Rev. A*, **39**, 2175.
- [10] POSCH, H. A., HOOVER, W. G., and HOLIAN, B. L., 1990, *Ber. Bunsenges phys. Chem.*, **94**, 250.
- [11] BORSZÁK, I., BARANYAI, A., and POSCH, H. A., 1996, *Physica A*, **229**, 94.
- [12] DELLAGO, CH., and POSCH, H. A., 1997, *Physica A*, **240**, 68.
- [13] KWON, H.-H., and PARK, B.-Y., 1997, *J. chem. Phys.*, **107**, 5171.
- [14] MEHRA, V., and RAMASWAMY, R., 1997, *Phys. Rev. E*, **56**, 2508.
- [15] ALLEN, M. P., FRENKEL, D., and TALBOT, J., 1989, *Comput. Phys. Rep.*, **9**, 301.
- [16] BELLEMANS, A., ORBAN, J., and VAN BELLE, D., 1980, *Molec. Phys.*, **39**, 781.
- [17] MILANOVIĆ, LJ., POSCH, H. A., and HOOVER, WM. G., 1998, *Chaos*, **8** (in the press).
- [18] DELLAGO, CH., POSCH, H. A., and HOOVER, W. G., 1996, *Phys. Rev. E*, **53**, 3694.
- [19] PESIN, JA. B., 1976, *Sov. Math. Dokl.*, **17**, 196.
- [20] HOOVER, W. G., BOERCKER, K., and POSCH, H. A., 1998, *Phys. Rev. E*, in press.
- [21] BENETTIN, G., GALGANI, L., GIORGILLI, A., and STRELCCYN, J.-M., 1980, *Meccanica*, **15**, 9.
- [22] WOLF, A., SWIFT, J. B., SWINNEY, H. L., and VASTANO, J. A., 1985, *Physica D*, **16**, 285.
- [23] VAN ZON, R., VAN BEIJEREN, H., and DELLAGO, CH., 1997, unpublished.
- [24] DELLAGO, CH., and POSCH, H. A., 1996, *Physica A*, **230**, 364.